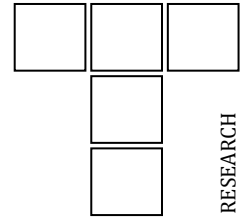


DOI: 10.24874/ti.1548.09.23.11

# Tribology in Industry

www.tribology.rs



## Heat Treatment Influence on the Cavitation Erosion Zn-Mg Behavior Used for Biomedical Applications

Alexandru Nicolae Luca<sup>a</sup>, Ilare Bordeasu<sup>a,b,\*</sup>, Cristina Maria Iordache<sup>c</sup>, Gabriela Ciungu<sup>c</sup>, Brandusa Ghiban<sup>c</sup>, Marian Miculescu<sup>c</sup>, Lavinia Madalina Micu<sup>d</sup>

<sup>a</sup>University Politehnica of Timisoara, Piata Victoriei no. 2, Timisoara, Romania,

<sup>b</sup>Romanian Academy of Scientists, Timisoara branch, Miahai Viteazul no.1, Timisoara, Romania,

<sup>c</sup>University Politehnica Bucharest, Splaiul Independentei no. 313, sector 6, Bucharest, Romania,

<sup>d</sup>University University Of Life Sciences "King Mihai I" From Timisoara, Calea Aradului no. 119, Timisoara, Romania.

### Keywords:

Zinc-magnezium alloy

Heat treatment

Microstructure

Cavitation erosion resistance

Depth and erosion rate

### ABSTRACT

Recent research in the medical field of temporary implants refers to the development of new biodegradable alloys, which are simultaneously subject to aggressive conditions of pressure fluctuations exerted in blood vessels. Both zinc and magnesium are biocompatible metallic materials, but also biodegradable. The present work approaches a new alloy from the Zn-Mg system, elaborated within the Polytechnic University of Bucharest, on which cavitation erosion tests were performed. It was followed the effect of applying the homogenization heat treatments of cast alloy, at different temperatures and maintenance durations (300 °C and 400 °C, each with a maintenance of 5h and 10 h) on the behavior at the vibratory cavitation. Finally, the correlation between the parameters of the heat treatment – the structure – behavior at cavitation erosion compared to those of the untreated thermal alloy was determined.

\* Corresponding author:

Ilare Bordeasu 

E-mail: [ilarica59@gmail.com](mailto:ilarica59@gmail.com)

Received: 13 September 2023

Revised: 16 October 2023

Accepted: 27 November 2023

© 2024 Published by Faculty of Engineering

### 1. INTRODUCTION

The medical literature [1] shows applications of zinc and magnesium as biodegradable and biocompatible metals. Studies by flow specialists (especially engineers and physicists) show that the blood circulatory system is similar to hydraulic pumping installations, in which the heart plays the role of the pump, and the veins, regardless of size, are assimilated to networks of branched pipes and loops [2-4]. So,

the blood circulatory system is one in which hydrodynamic phenomenon specific to pumping hydraulic installations can develop. As the most dangerous phenomenon, as shown by old and new studies [2,5-11], for the proper functioning and for the lifetime of some components in industrial installations that work in difficult-to-controllable hydrodynamic regimes, is cavitation, in recently, in the medical field [3,4,12], studies are being developed that analyze the blood circulatory system as one

similar to that in machines and hydraulic installations. The difference is the liquid environment (blood) and the medical causes that generate, in various areas, sudden pressure fluctuations, from vaporization to very high values, especially at the entrance and exit of the heart, with harmful effects on the individual's physical health. These manifestations can cause, through the specific mechanism of cavitation [2,5,10,11], to break the vessels and even cracks in the walls of the heart.

As a result, for the health and reduction of hydrodynamic, harmful effects of blood circulation or heart function, the insertion of stents and the replacement of heart valves with suitable devices made of biocompatible and biodegradable materials has become a leading area of engineering and medical research in the field of cardiovascular surgery [1,3,12,13].

In this direction is the research, new from our point of view, carried out on a new biodegradable ZnMg alloy created in the Specialized Laboratory of the Politehnica University of Bucharest, whose performance under cavitation demands is studied in the Cavitation Erosion Research Laboratory of the University Timisoara Polytechnic. The goal is to use the alloy in stents and heart valves, so that the health status of the individual becomes normal, and the lifetime of the devices implanted in the blood circulatory system is as long as possible, without endangering life.

## 2. RESEARCH MATERIAL AND METHODOLOGY

### 2.1 The research material

In this work, an alloy from the Zn-Mg system was developed, in a crucible flame furnace at 650°C, using elements of advanced purity, respectively Zn 99.99%, magnesium 99.99% and calcium 99.99%. Casting was done in stainless steel ingot. The resulting chemical composition was Zn = 97.68%; Mg = 1.458%; Fe= 0.589%; Mn = 0.086%; Cu= 0.09%; Si= 0.065%; Al=0.032%. Two homogenization thermal treatments were performed on the cast alloy at 300°C and 400°C, each with a holding time of 5 hours and 10 hours, respectively. The thermal treatments were carried out in a Nabertherm oven. Microstructural investigations were carried out

on the experimental samples to identify the phases and microstructural constituents and the mechanical characteristics were determined.

### 2.2 Apparatus and cavitation test method

The test program for cavitation erosive stresses was carried out in the Cavitation Erosion Research Laboratory of the Politehnica University of Timișoara, on the standard vibrating device with piezoceramic crystals, fig. 1 [5,14]. The tests carried out comply with the procedural requirements described in the international standard ASTM G32-2016, but also with the stages of the laboratory's custom, regarding the total duration of 165 minutes and the 12 intermediate durations (one each of 5 and 10 minutes and 12 of 15 minutes each ), to the method of preparation and storage of the samples at the end of the test, to the recording of mass losses, related to the intermediate periods, to the processing and interpretation of data that do not contradict the requirements described in ASTM G32-2016 [5,14,15].

The liquid medium used was distilled (deionized) water, whose temperature, during the intermediate period, was  $22 \pm 10^\circ\text{C}$ .

The working parameters of the vibrator, which influenced the intensity of the cavitation stresses through the erosive act of the structure of the cavity surfaces, are subjected to rigorous control and maintained at the values recommended by ASTM G32-2016, as a result of the program being run by the computer, through a software built within the laboratory [1,6,16-18].

Their values are: electric power developed by the electronic ultrasound generator = 500 W, vibration amplitude = 50  $\mu\text{m}$ , vibration frequency = 20  $\mu\text{m} \pm 0.1$  kHz. For the accuracy of the research results, 3 samples were tested from each heat treatment regimen.

The test method is the vibratory one with a stationary sample, fig. 2b. The sample mounted in the vibrating mechanical system, which generated the erosion on the surface of the stationary sample, is made of STELLITE type stainless steel, known to be one with very high resistance to the erosion produced by the cyclic stresses of the microjets generated by the hydrodynamics of the vibrating cavitation [5,11,16-20].

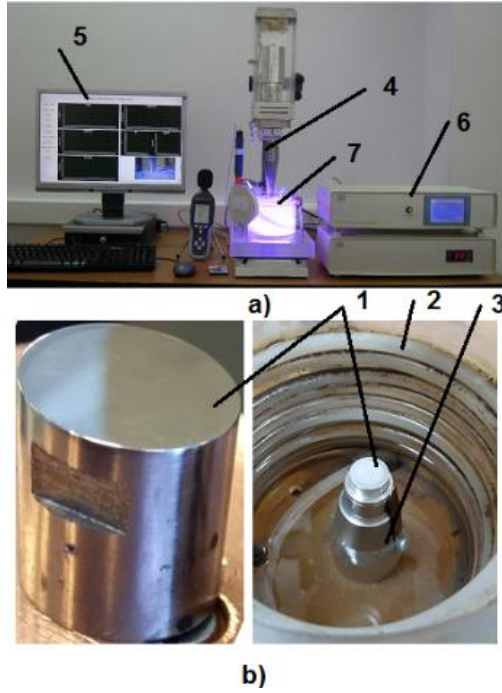


**Fig. 1.** Image and details of experimental stand composition: a) image of the vibrator assembly; b) sample details and fixture; 1. sample subjected to cavitation; 2. coil cooling distilled water; 3. the sample fixation device; 4. mechanical vibrating system; 5. screen displaying the parameters controlled during cavitation; 6. electronic ultrasound generator; 7. the vessel with distilled water.

Before starting the cavitation tests, the surfaces of the samples, which were to be tested, according to the laboratory's custom and the provisions of ASTM G32-2016, were polished to a roughness  $R_a = 1.6 \dots 0.8 \mu\text{m}$ .

Based on the mass losses, determined after each intermediate test period, the experimental values of the mean depths of erosion (MDE) and their related velocities (MDER) were determined and, respectively, pictures of the eroded surface were taken with the device Canon Power Shot A 480 (see figs. 8 and 13) to follow the destruction of the structure through elasto-plastic deformations and through the evolution of the dimensions of the caverns, as an expression of the behavior and resistance of the structure to the cyclic fatigue stresses of shock waves and cavitation microjets created by the implosion bubbles.

The average erosion depths and related velocities were determined with the relations:

$$\Delta MDE_i = \frac{4 \cdot \Delta m_i}{\rho \cdot \pi \cdot d_p^2} [\mu\text{m}] \quad (1)$$

$$MDER_i = \Delta MDE_i / \Delta t_i [\mu\text{m}/\text{min}] \quad (2)$$

where:

$i$  - represents the testing period;

$\Delta m_i$  - is the mass of material, lost through erosion, in period  $i$ , in grams;

$\rho$  - the density of the Zn-Mg alloy, in  $\text{g}/\text{mm}^3$ ;

$\Delta t_i$  - duration of the intermediate period " $i$ " of cavitation (of 5, 10 and 15), in minutes;

$d_p$  - diameter of the sample surface, subject to cavitation attack ( $d_p = 15.8 \text{ mm}$ );

$\Delta MDE_i$  - the value of the average depth of erosion achieved by cavitation in the period  $\Delta t_i$ .

For the construction of the specific diagrams, which contain the experimental values and the averaging curves, of an analytical form, with the parameters determined statistically based on the experimental values, necessary for the analysis of the behavior and resistance (destruction) of the surface structure to the cavitation stresses, the relations below were used:

- for the cumulative average depth obtained on the basis of experimentally determined mass values after each intermediate period:

$$MDE_i = \sum_{i=1}^{13} \frac{4 \cdot \Delta m_i}{\rho \cdot \pi \cdot d_p^2} [\mu\text{m}] \quad (3)$$

- for the analytical curve averaging the experimental values of the cumulative average depth of erosion penetration [19,20]

$$\begin{aligned} MDE(t) &= A \cdot t \cdot (1 - e^{-B \cdot t}) \\ \text{or} \\ MDE(t) &= A \cdot t \cdot (1 + e^{-B \cdot t}) \end{aligned} \quad (4)$$

- for the analytical curve averaging the experimental values obtained for the average erosion penetration velocities, determined over the intermediate periods [19,20]

$$MDER(t) = A \cdot (1 - e^{-B \cdot t}) + A \cdot B \cdot t \cdot e^{-B \cdot t} \quad (5)$$

where:

for  $i = 1 \Delta t_i = 0$

$A$  - is the scale parameter, statistically established on the basis of experimental values, for constructing their approximation/averaging curve, provided that their deviations from it are minimal;

$B$  - is the shape parameter of the curve, established statistically based on experimental values.



The values of the parameters A and B were made in the Matchad program, following a model built in the Cavitation Erosion Research Laboratory [5,14,19,20].

As a result of the complexity of the hydrodynamics of cavitation and the dependence of the resistance of the required surface structure on a multitude of factors (microstructural defects, type of microstructure, chemical composition, physical-mechanical properties, etc.) the tolerance ranges accepted for this type of stress are from 99% to 90%, whose upper limits "S" and lower "I" are calculated as follows [5,14,21]:

- for the 99% tolerance Interval:

$$S99(t) = MDE(t) + 1 \cdot \sigma ; I99(t) = MDE(t) - 1 \cdot \sigma \quad (6)$$

- for tolerance interval 95%:

$$S90(t) = MDE(t) + 10 \cdot \sigma ; I90(t) = MDE(t) - 10 \cdot \sigma \quad (7)$$

Where  $\sigma$  represents the average standard deviation of the experimental values compared to the MDE(t) averaging curve.

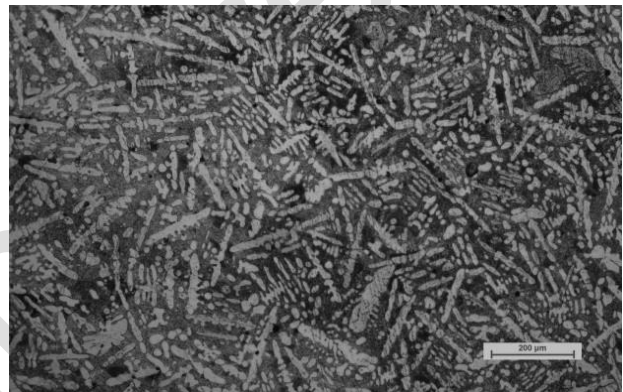
The dispersions of the experimental values, compared to the averaging curves and within the tolerance ranges, are the expression of the accuracy of the cavitation tests on the three samples, regardless of the state of the samples. Also, the width of the dispersion band, with the tolerance interval, from our experience and the analyzes performed on a series of data provided by the published works [10,11,14,16-18,21] as well as the values of the standard deviations  $\sigma$  show whether the test was conducted correctly, the procedural steps were respected, and the parameters of the vibrator, which determined the destructive intensity of the cavitation, were very well controlled.

For the ease of presentation, description, analysis and understanding of the research results in this chapter, the symbolizations below will be used. So: 300/5 – the structure obtained by treatment with a temperature of 300 °C with a holding time of 5 hours, 300/10 – the structure obtained by treatment with a temperature of 300 °C with a holding time of 5 hours, 400/5 – the structure obtained by treatment with a temperature of 300 °C with a holding time of 5 hours, 400/5 – the structure obtained by treatment with a temperature of 300 °C with a holding time of 10 hours.

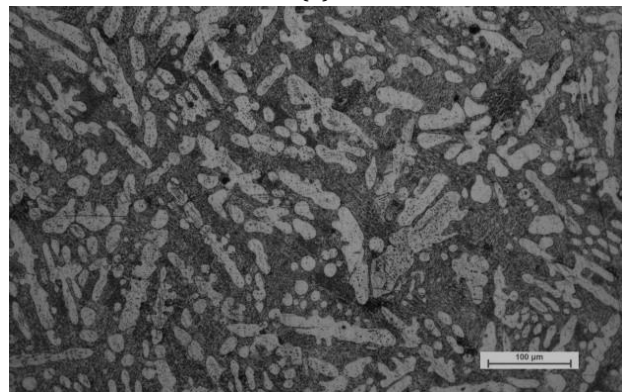
### 3. EXPERIMENTAL RESULTS. ANALYSIS AND DISCUSSIONS

#### 3.1 Structural analysis and mechanical behavior

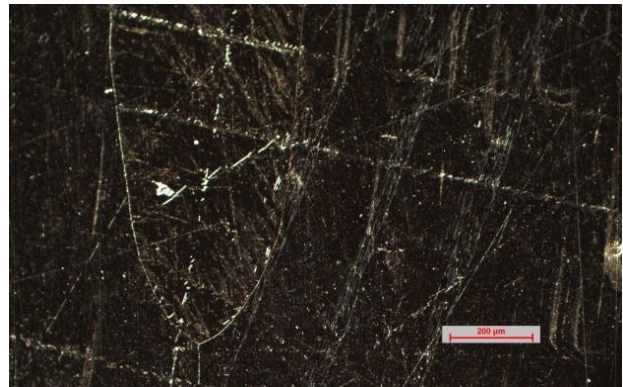
The alloy from the Zn-Mg system is an alloy formed from solid solution based on zinc  $\alpha$  and an intermetallic compound  $Mg_{2}Zn_{11}$ . The cast structures have dendritic segregation, where the dendritic arms are considerably influenced both by the homogenization temperature after casting, respectively 300°C or 400°C, and especially by the duration of holding at the respective temperatures. Thus, after homogenization at 300°C/5 hours (fig. 2a,b) the structure is formed by an inhomogeneous solid solution of zinc, with interdendritic separation of intermetallic compounds  $Mg_{2}Zn_{11}$ .



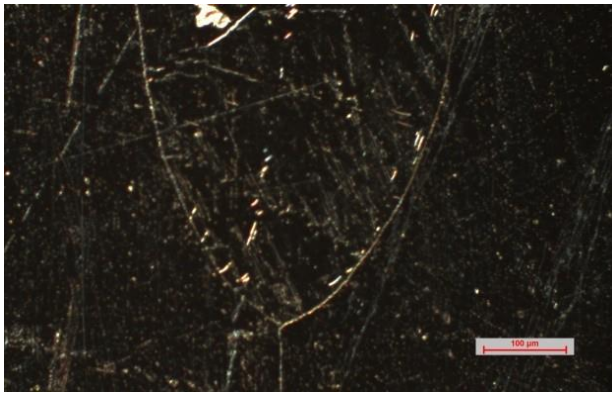
(a)



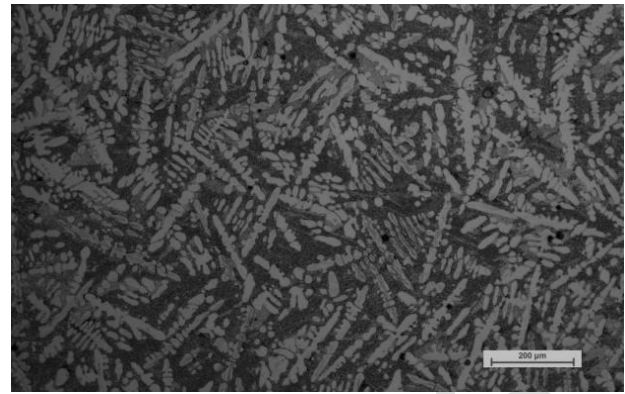
(b)



(c)



(d)

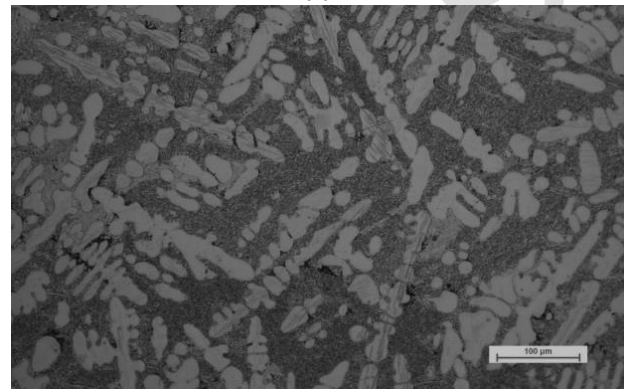


(a)

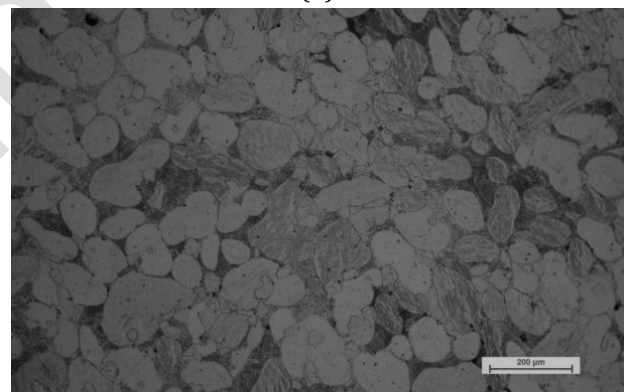
**Fig. 2.** Structural analysis of Zn-Mg alloy specimens, after homogenization at 300°C, 2% nital attack, and different holding times: (a)- 5 hours, (b) - detail of image (a), (c) - 10 hours, (d) - detail of image (c).

The arms of the dendrites are located in the range of 100-180  $\mu\text{m}$ , with a chaotic arrangement in the metal matrix. When the homogenization time increases to 10 hours (fig. 2c,d), there is an exaggerated growth of the grains, with the elimination of the dendrites. The application of a homogenization at a temperature of 400°C/5 hours (fig. 3a,b) leads to the formation of an inhomogeneous solid solution of zinc with the interdendritic existence of intermetallic compounds of  $\text{Mg}_2\text{Zn}_{11}$ , in which, however, the dendritic arms have smaller dimensions, in the range of 80-150  $\mu\text{m}$ . When the holding time increases to 10 hours, the dendrites are almost completely removed, with the spheroidization of the arms and the intergranular arrangement of the compounds  $\text{Mg}_2\text{Zn}_{11}$  (fig. 3c,d).

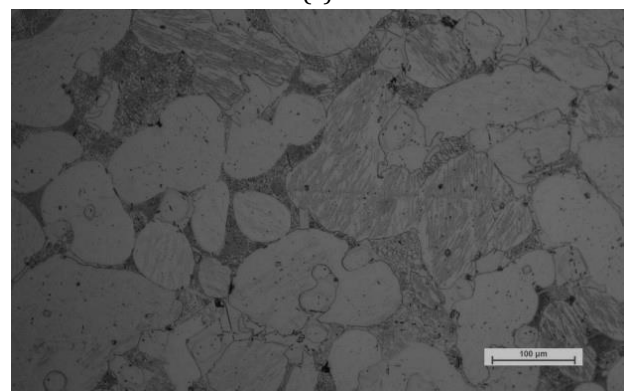
The results of the determination of the HB hardness characteristics are shown in table 1. It is noted that by applying the homogenization treatments, different hardness values are obtained depending on the temperature and duration of the homogenization treatment. If, when applying a homogenization treatment at 300°C / 5 hours, the HB hardness values are the highest, respectively 76, when the homogenization time increases, the values decrease drastically, to 57 HB. Applying a homogenization at 400°C makes the hardness values of the samples to be in the range of 60-70HB.



(b)



(c)



(d)

**Fig. 3.** Structural analysis of Zn-Mg alloy samples, after homogenization at 400°C, 2% nital attack, and different holding times: (a)- 5 hours, (b)- detail of image (a), (c)- 10 hours, (d)- detail of image (c).



**Table 1.** Brinell hardness values of Zn-Mg alloy samples in different structural states.

Alloy	Molded and homogenized state	Hardness HB
Zn-Mg	300°C/ 5h	76
	300°C/ 10h	57
	400°C/ 5h	62
	400°C/ 10h	68

### 3.2 Analysis of cavity behavior after thermal treatment at 300 °C

In fig. 4-7 are given the diagrams that characterize the behavior and resistance of the structures of the surfaces treated at 300 °C, affected by the cavitation erosion generated by the vibrator, recommended for analysis by ASTM G32-2016 and used in our analyzes.

In these diagrams, the values of parameters A and B are displayed, as well as the reference parameters  $MDE_{max}$ , and MDERs, erosion characteristics, which, by comparison, show the resistance of the structure to the stresses of cavitation microjets.

Fig. 4 and 6, by the dispersion bands of the experimental values against the  $MDE(t)$  averaging curves, with tolerance of 98% and 97%, respectively by the values of the average standard deviations  $\sigma$  of 0.811 and 0.123 certify the accuracy of the research from the point of view of control rigorously throughout the experimental program, with maintenance within the operating limits of the values of the parameters that characterize the hydrodynamics of the vibrating cavitation (electronic generator power, vibration amplitude and frequency, liquid medium temperature).

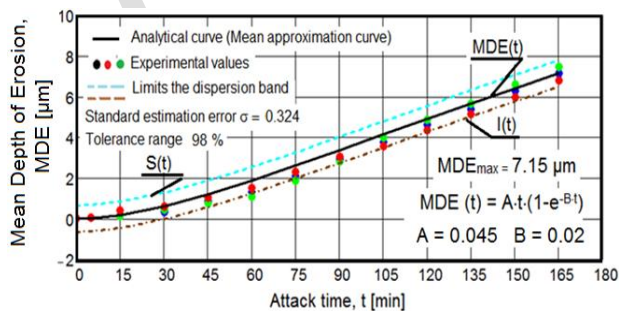


**Fig. 4.** Variation of cumulative average depth with duration of cavitation(300/5h).

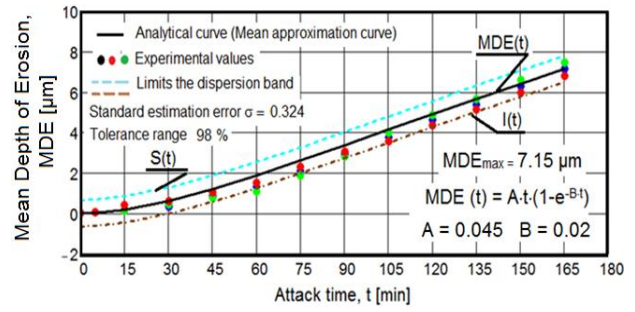


**Fig. 5.** Variation of average erosion penetration velocity with cavitation duration (300/5h).

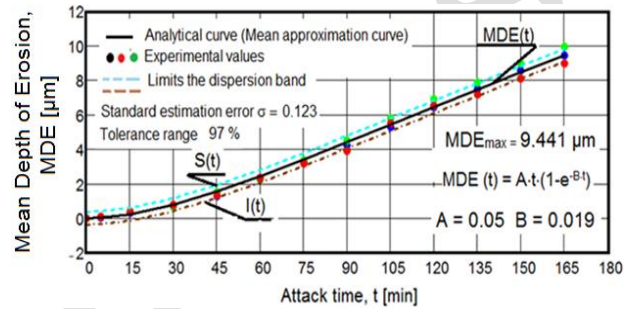


**Fig. 6.** Variation of cumulative average depth with duration of cavitation (300/10h).

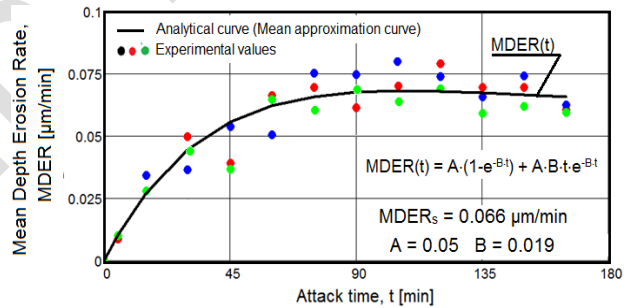


**Fig. 7.** Variation of cumulative average depth with duration of cavitation (300/10h).

The dispersion of the experimental MDE and MDER values, the evolution forms of the  $MDE(t)$  and  $MDER(t)$  averaging curves and the values of the reference parameters  $MDE_{max}$  and MDERs show important aspects for the behavior of the components made of this alloy, with these types of heat treatment, of type of stents and valves used in cardiology, from the point of view of the hydrodynamics of blood circulation in the human body, as a result of pressure fluctuations. Therefore, it is found:

1. Insignificant differences between the experimental values, obtained on the three samples, regardless of the duration of the heat treatment, which indicates that the heat treatment regimen was correctly carried out;

2. Slight differences, natural, between the dispersions of the MDER speed values compared to the averaging curves, caused by the values of the mechanical properties (HB hardness-table 1) and the duration of the heat treatment regime;
3. Increases of 32% between the values of  $MDE_{max}$  and of about 35% between the values of MDERs (the value reached by the MDER(t) curve at 165 minutes - known as the rate of stabilization of erosion [5,15,14,21]), determined by the increase in the duration of maintenance at 10 hours, with a direct effect on increasing the resistance of the structure to the impact with cavitation microjets and, obviously, with a direct effect on increasing the life of possible parts such as valves and cardiological stents;
4. The similar evolutions of the MDER(t) curves, from figs 4 and 6, show that from the point of view of the potential energy absorption, created by the impact pressure with the microjets and shock waves, the two surfaces (see also the images from fig. 8) behave similarly, the difference in resistance being given by the values of the mechanical properties and microstructure, an important aspect for the behavior of stents and valves in people with heart problems.

In fig. 8 photographic images from 4 durations of the cavitation attack are shown.

According to the dimensions of the caverns and the evolution of the eroded area in the cavitated surface, the superior resistance of the structure resulting from the 300/5 treatment results.

Also, the images confirm the behavior under cavitation stresses, confirming the statements made on the basis of the diagrams in fig. 4...7. The shape of the caverns in these images, supplemented by the microscopic images in fig. 9 shows that the sizes of the grains ejected upon impact with cavitation microjets are small, specific to structures with high resistance to cavitation stress [5,10,22] which, through biodegradation, they can quickly dissolve in the blood circulatory system, so the life of devices used in cardiovascular surgery is long and not life-threatening.

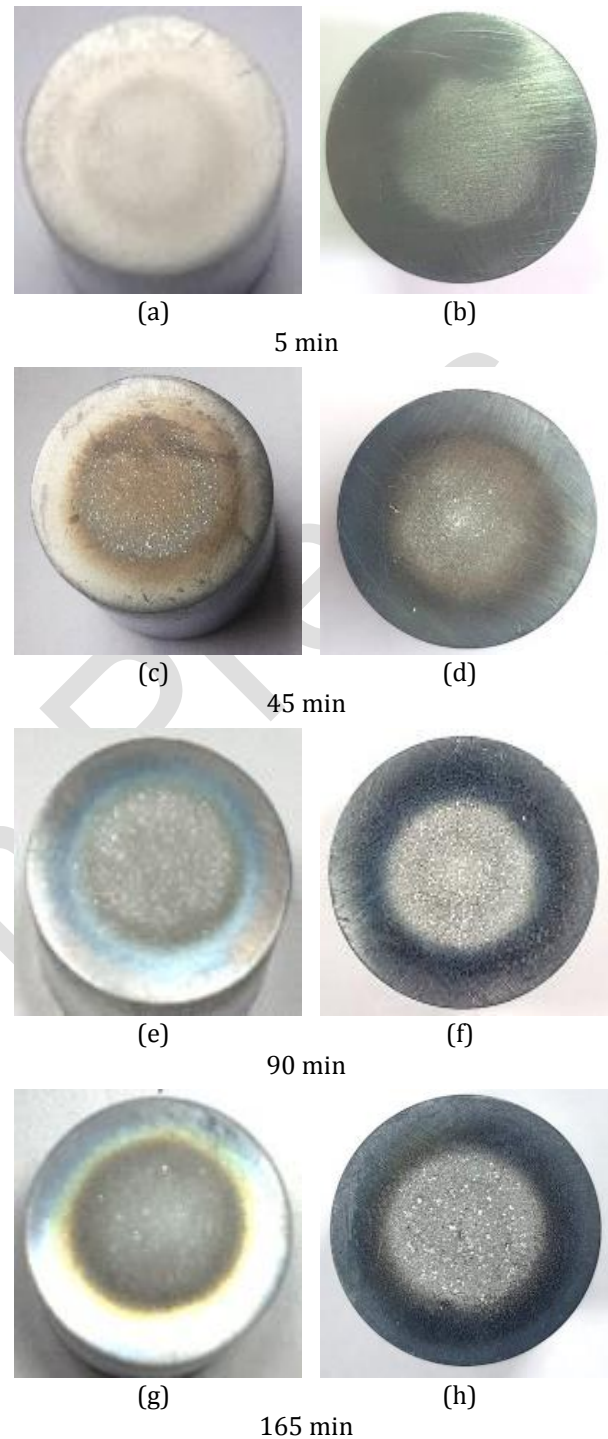


**Fig. 8.** Macrofractographic images after different durations of cavitation attack: 300/5h (a, c, e, g); 300/10h (b, d, f, h).

The results of the stereomacrostructural analysis are shown suggestively in the images in fig. 9, as well as in table 2. It is noted that the surface attacked by cavitation in the samples homogenized at 300°C is quite large and differentiated by the duration of the homogenization. Thus, after 5h homogenization, the surface with cavitation erosion is in large



proportion, 74%, and the surface most affected by the cavitation attack is about 63%. The aspects captured at 25x magnification show a fragile, shiny crystalline aspect, with flattened cavities. When

the homogenization time increases to 10 hours, the aspects become more intense, with much larger cavities, and with a surface of about 81% affected by the cavitation attack.

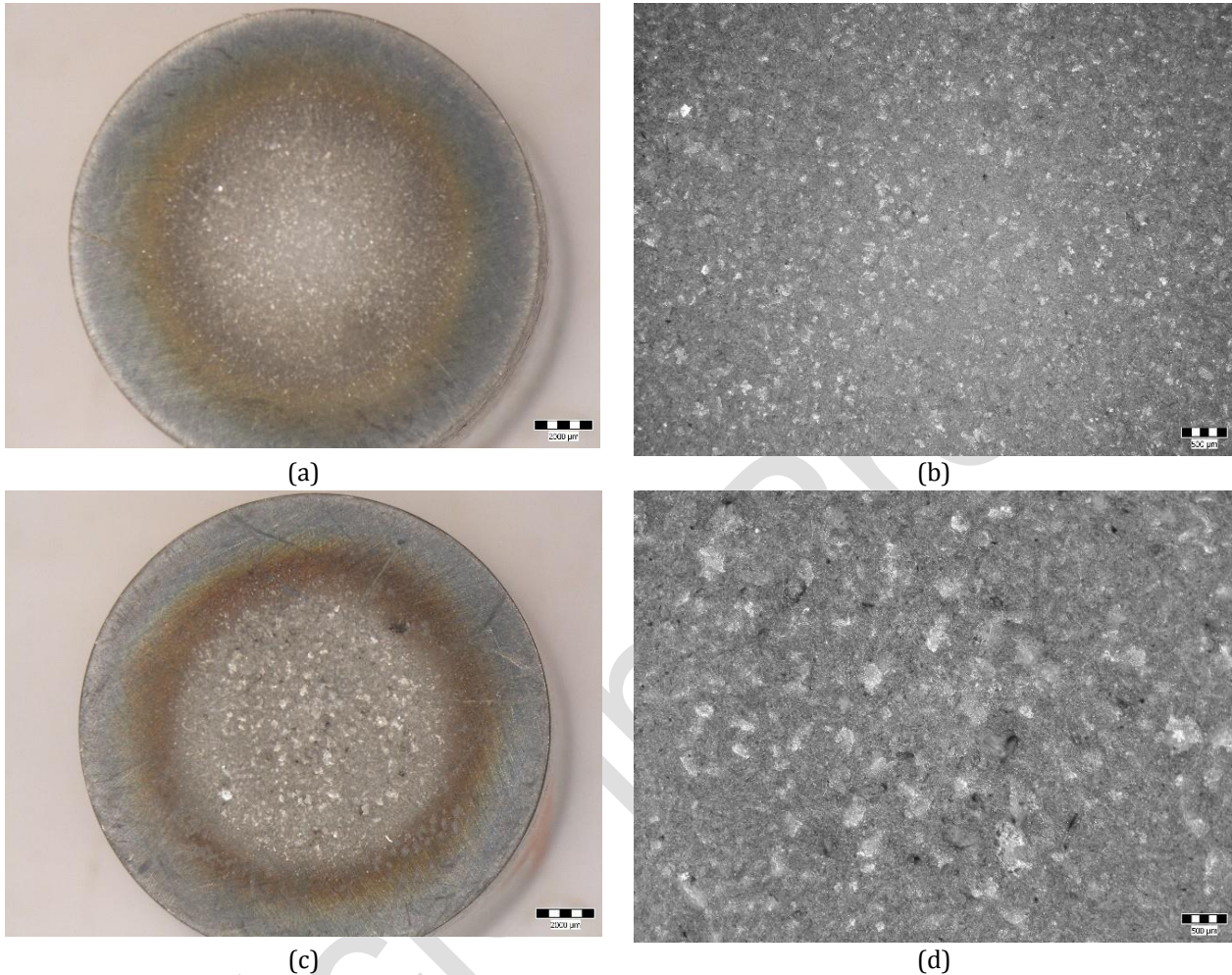


**Fig. 9.** The macrostructural aspect of the surfaces after cavitation erosion testing of Zn-Mg alloy samples, after homogenization at 300°C and different holding times: (a, c) - x8; (b, d) - x25; (a, b) - 5 ore; (c, d) - 10 ore.

**Table 2.** The results of the measurements regarding the dimensions of the areas affected by the cavitation erosion of the Zn-Mg alloy specimens in different structural states.

Alloy, condition	Diameter of the specimen, mm	d <sub>1</sub> mm	d <sub>2</sub> mm	$\frac{\pi d_1^2}{\pi d_p^2}$ %	$\frac{\pi d_2^2}{\pi d_p^2}$ %
Zn-Mg, 300°C/5h	16024	11800	10141	74	63
Zn-Mg, 300°C/10h	15592	12695	9658	81	61
Zn-Mg, 400°C/5h	15866	10704	5160	67	33
Zn-Mg, 400°C/10h	15910	9334	4194	59	26

d<sub>1</sub>- The diameter of the area affected by the cavity; d<sub>2</sub>- The diameter of the most affected cavity area; d<sub>2</sub>- The diameter of the most affected cavity area; d<sub>p</sub>= 15.8 mm- The diameter of the sample surface, subject to cavitation attack.

### 3.3 Analysis of cavity behavior after thermal treatment at 400 °C

In fig. 10...13 are given the diagrams that characterize the behavior and resistance of the structures of the surfaces treated at 400 °C.

As with the 300 °C treatment, fig. 10 and 12, through the dispersion bands of the experimental values against the MDE(t) averaging curves, also with a tolerance of 98% and 97%, respectively through the values of the average standard deviations  $\sigma$ , of 0.084 and 0.042, the accuracy of the research is certified from the point in view of the rigorous control throughout the experimental program as a result of the control and management of the experiment through the software used.



And these diagrams contain the values of parameters A and B and of the reference ones for the characterization of resistance to cavitation erosion ( $MDE_{max}$  and  $MDERs$ ).

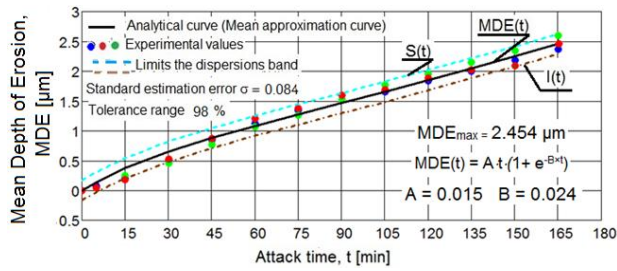


**Fig. 10.** Variation of the cumulative average depth with cavitation duration (400/5h).

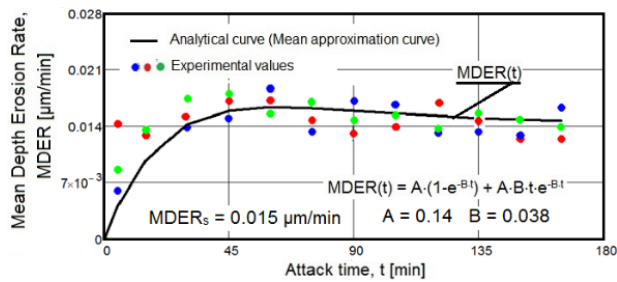


**Fig. 11.** Variation of cumulative average depth with cavitation duration (400/5h).

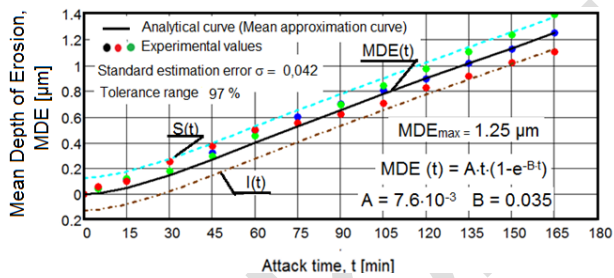


**Fig. 12.** Variation of the cumulative average depth with the duration of cavitation (400/10h).

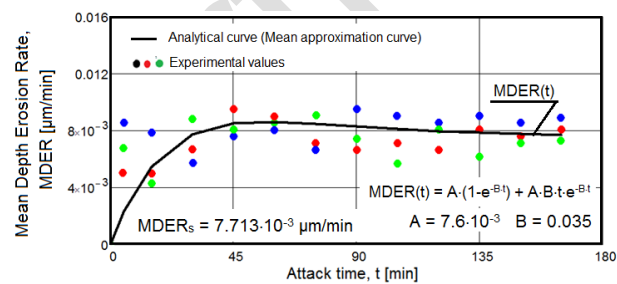


**Fig. 13.** Variation of the cumulative average depth with the duration of cavitation (400/10h).

Proceeding similarly to the analysis made in fig. 2...7, from the analysis of the data from the diagrams shown in fig. 10...13 result in similar conclusions, regardless of the duration of the treatment (5 or 10 hours), in terms of the dispersion of the experimental values compared

to the  $MDE(t)$  or  $MDER(t)$  mediation curves and the differences between the three samples of each heat treatment regimen.

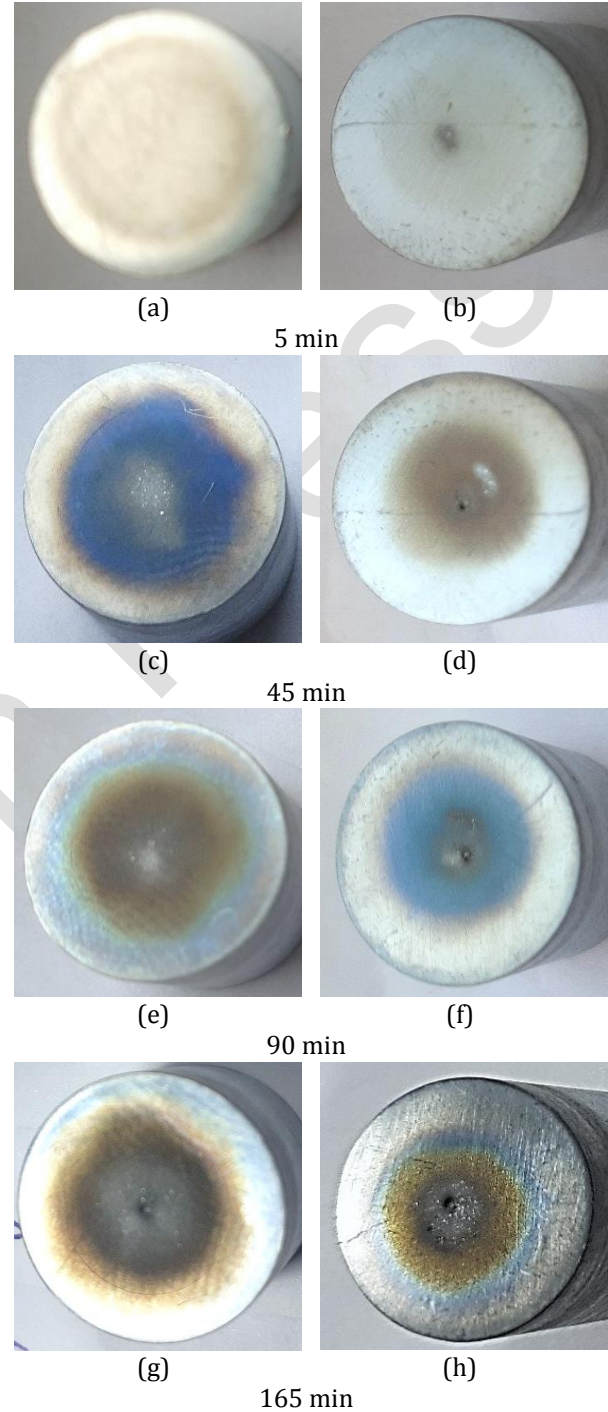


**Fig. 14.** Macrofractographic images after different durations of cavitation attack: 400/5h (a, c, e, g); 400/10h (b, d, f, h).

From the point of view of the structure's resistance to the hydrodynamic stresses of cavitation, through the 10-hour regime, compared to the 5-hour regime, an increase of about 96% is obtained, if we refer to the values of  $MDE_{max}$  and of about 97%, if we refer to  $MDERs$  values. So for the temperature of

400 °C, the duration of 10 hours offers the longest lifetime of the components made of ZnMg alloy and used in cardiovascular surgery on the blood circulatory route. We consider that the difference in resistance is also caused by the differences between the microstructures resulting from the durations of holding at 400 °C and those between the values of the mechanical properties (table 1).

Here too, the similar evolutions of the MDER(t) curves can be observed, showing that, from the point of view of the absorption of the potential energy created by the impact pressure with the microjets and the shock waves, the two surfaces (see also fig. 14) behave similarly, the difference in resistance being also given by the values of the mechanical properties and microstructure, an important aspect for the behavior of cardiac stents and valves (valves), made of this alloy.

In fig. 14, photographic images are shown, for each of the three tested samples, from 4 significant times, which show the evolution of the cavitation erosion in depth and as an extension in the surface area required by the cavitation microjets.

The photographic images in fig. 14 are consistent with the values obtained for the average depth of erosion (MDE) and for the average rate of penetration of erosion (MDER) and with those stated in the analysis based on the diagrams in fig. 10...13. Regardless of the reference type, these photographic images confirm that the structure resulting from heat treatment 400/10 behaves better than that obtained from heat treatment 300/5.

The results of the stereomacrostructural analysis are shown suggestively in the images in fig. 15, as well as in table 2. It is noted that the surfaces attacked by cavitation in the samples homogenized at 400°C are much smaller and differentiated by the duration of maintenance during homogenization compared to the same surfaces after homogenization at 300°C. Thus, after homogenization at 400°C/5h, the surface with cavitation erosion is in a smaller proportion, respectively 67%, and the surface most affected by the cavitation attack is only 33%.

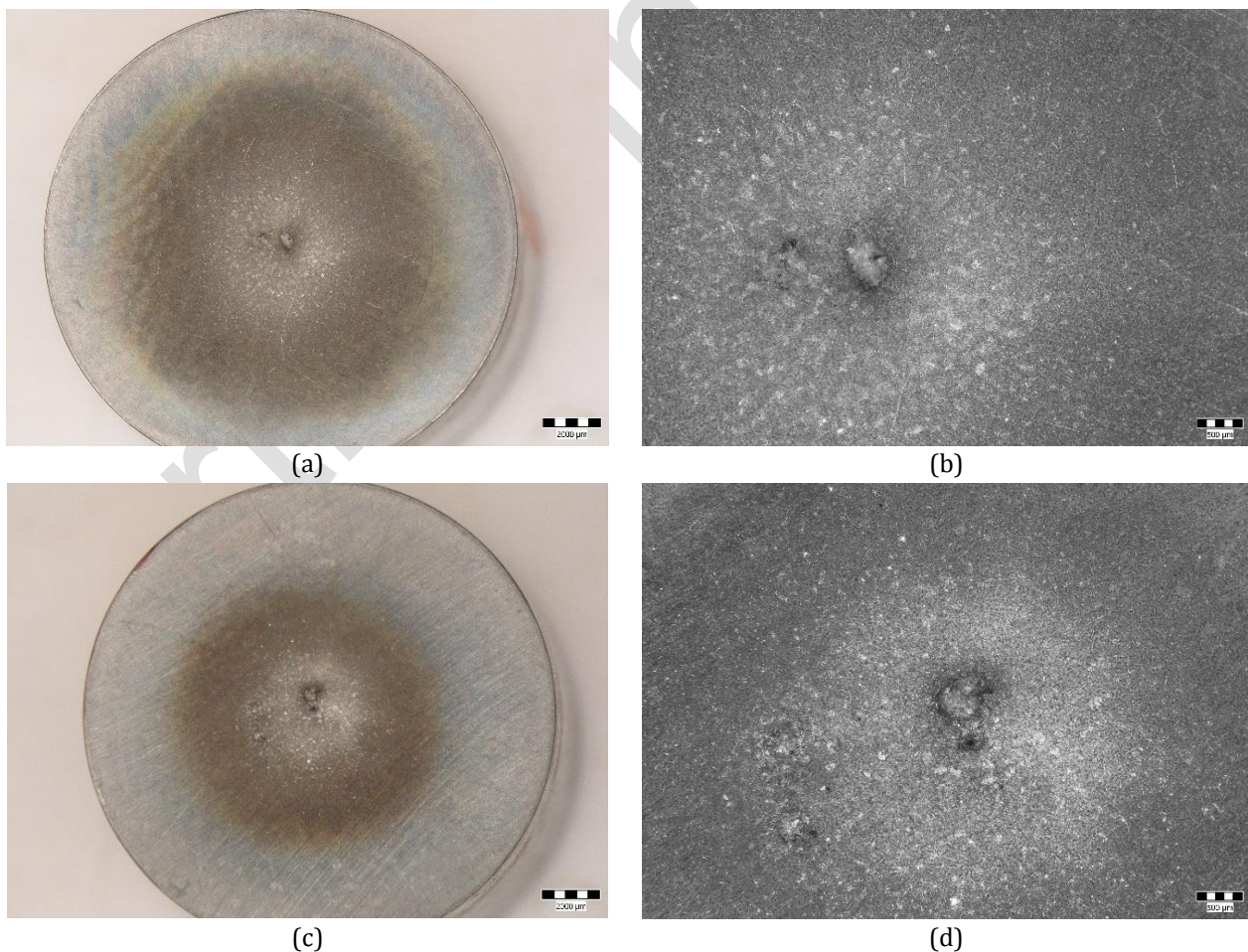


**Fig. 15.** The macrostructural aspect of the surfaces after cavity erosion testing of other Zn-Mg samples, after homogenization at 400°C and different holding times: (a, c) - x8; (b, d) - x25; (a, b) - 5 hours; (c, d) - 10 ore.



The aspects captured at 25 times magnification show the same fragile, shiny crystalline appearance, with flattened cavities, but of reduced size. When the homogenization time increases to 400°C/10 hours, the surface with cavitation erosion is in a lower proportion, namely 59%, and the surface most affected by the cavitation attack decreases to only 26%. The reduced dimensions of the caverns that appeared during the cavitation stress (given by a more dendritic structure, which is eliminated as the homogenization time increases) confirm the beneficial effect of the thermal treatment, on the resistance of the structure to the erosive stresses of cavitation, especially since the mass of the ejected grain, due to biodegradation, it does not endanger the lives of cardiac patients with stent implants or valves made of this alloy.

### 3.4 Comparison of resistances to vibratory cavitation erosion

The histogram in fig. 16 shows the differences between the values of the  $MDE_{max}$  and  $MDER_s$  parameters as an expression of the effect of the heat treatment regime on the resistance of the surface structure to cavitation stresses.

From the point of view of the effect of these treatments on the elements used in operative cardiology, such as stents or valves, the histogram is a benchmark for choosing the best technological solution for the treatment of the ZnMg alloy, depending on the severity of the subject with heart disease, on the signals recorded in blood pressure fluctuations.

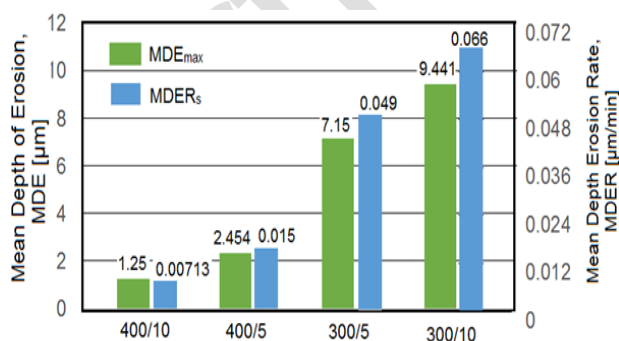


**Fig. 16.** Comparison of values of reference parameters of resistance to cavitation.

From the point of view of the structure's resistance to vibratory cavitation erosion, the histogram data show that the highest resistance is conferred by the 400/10 treatment, which:

- according to the  $MDER_s$  parameter values, compared to the 300/5 treatment, it is about 6.8 times higher, and compared to the 300/10 treatment, it is about 9.3 times higher;
- according to the values of the  $MDER_{max}$  parameter, compared to the 300/5 treatment it is about 5.7 times higher, and compared to the 300/10 treatment it is about 7.6 times higher.

The increase in strength conferred by the 400/5 heat treatment compared to the 300 °C heat treatment is:

- about 3.3 times higher according to the values of  $MDER_s$  and about 3 times according to the values of  $MDE$ , for the maintenance duration of 5 hours;
- about 4.4 times higher according to  $MDER_s$  values and about 3.8 times according to  $MDE$  values, for the maintenance time of 10 hours.

## 4. CONCLUSIONS

The lifetime of the biodegradable ZnMg alloy, used in the manufacture of stents and valves intended for cardiovascular surgery, to mitigate the effects caused by pressure oscillations in the blood circulatory system, which can generate hydrodynamic phenomena specific to cavitation, can be increased by applying a volume thermal treatment, correctly defined by temperature and holding time.

The results of the present paper show that, by applying different homogenization treatments to the structures cast from Zn-Mg alloy, significant improvements in the resistance to cavitation attack can be made. The obtained results show that the application of a homogenization at 400°C leads to structures and mechanical properties that confer resistance to cavitation erosion (3...9.3) times higher than those obtained by thermal treatment at 300 °C, regardless of the holding times (5 hours or 10 hours).

The increase in resistance to cavitation attack is given by obtaining some structures where dendritic segregation disappears, obtaining solid solutions of zinc with spheroidized dendrites and the intergranular presence of  $Mg_2Zn_{11}$  compounds. The increase in temperature and duration of maintenance are also advantageous due to the very small dimensions of the material

ejected from the surface subjected to the impact pressures created by the cavitation microjets, which can quickly degrade without blocking blood circulation, with the production of other phenomena specific to non-permanent movement, battering ram type and with a high degree of turbulence, which can endanger the cardiovascular integrity of the individual.

## REFERENCES

- [1] Y.F. Zheng, X.N. Gu, F. Witte, *Biodegradable metals*, Mater. Sci. Eng. R 77, pp. 1–34, 2014, doi: [10.1016/j.mser.2014.01.001](https://doi.org/10.1016/j.mser.2014.01.001)
- [2] I. Anton, *Cavitatie, Vol II*, Editura Academiei RSR, Bucuresti, 1985
- [3] E. Mostaed, M. Sikora-Jasinska, A. Mostaed, S. Loffredo, A.G. Demir, B. Previtali, D. Mantovani, R. Beanland, M. Vedani, *Novel Zn-based alloys for biodegradable stent applications: design, development and in vitro degradation*, J. Mech. Behav. Biomed. Mater. vol.60, pp. 581–602, 2016, doi: [10.1016/j.jmbbm.2016.03.018](https://doi.org/10.1016/j.jmbbm.2016.03.018)
- [4] W. Pachla, S. Przybysz, A. Jarzębski, M. Bieda, K. Sztwiertnia, M. Kulczyk, J. Skiba, *Structural and mechanical aspects of hypoeutectic Zn–Mg binary alloys for biodegradable vascular stent applications*, Bioactive Materials vol.6, pp.26–44, 2021, doi: [10.1016/j.bioactmat.2020.07.004](https://doi.org/10.1016/j.bioactmat.2020.07.004)
- [5] I. Bordeasu, *Monografia Laboratorului de Cercetare a Eroziunii prin Cavitate al Universitatii Politehnica Timisoara (1960-2020)* Editura Politehnica, Timisoara, Romania, 2020
- [6] I. Bordeasu, M. O. Popoviciu, I. Mitelea, V. Balasoiu, B. Ghiban, D. Tucu, *Chemical and mechanical aspects of the cavitation phenomena*, Revista de Chimie. 2007, vol. 58, no.12, pp. 1300-1304, 2007
- [7] L.M. Micu, I. Bordeasu, M.O. Popoviciu, M. Popescu, D. Bordeasu, L.C.Salcianu, *Influence of volumic heat treatments upon cavitation erosion resistance of duplex X2CrNiMoN 22-5-3 stainless steels*, in International Conference on Applied Sciences 2014 (ICAS2014), 2-4 October 2014, vol.85, art. number.012019, 2015
- [8] D. Bordeasu, O. Prostean, C. Hatiegan, *Contributions to Modeling, Simulation and Controlling of a Pumping System Powered by a Wind Energy Conversion System*, Energies, vol.14, no. 22, art. Article Number 7696, 2021, doi: [doi.org/10.3390/en14227696](https://doi.org/10.3390/en14227696)
- [9] D. Bordeasu, O. Prostean, I. Filip, F. Dragan, C. Vasar, *Modelling, Simulation and Controlling of a Multi-Pump System with Water Storage Powered by a Fluctuating and Intermittent Power Source*, Mathematics, vol. 10, no. 21, 2022, doi: [doi.org/10.3390/math10214019](https://doi.org/10.3390/math10214019)
- [10] J. P. Franc, J. M. Michel, *Fundamentals of cavitation*, Kluwer Academic Publishers-Dordrecht/Boston/London, 2004
- [11] R. Garcia, *Comprehensive Cavitation Damage Data for Water and Various Liquid Metals Including Correlation with Material and Fluid Properties*, Technical Report No. 6, University of Michigan, 1966
- [12] T. Huang, Y.F. Zheng, Y. Han, *Accelerating Degradation Rate of Pure Iron by Zinc Ion Implantation*, Regen. Biomater, 3 pp. 205–215, 2016, doi: [10.1093/rb/rbw020](https://doi.org/10.1093/rb/rbw020)
- [13] H. Li, H. Yang, Y. Zheng, F. Zhou, K. Qiu, X. Wang, *Design and characterizations of novel biodegradable ternary Zn-based alloys with IIA nutrient alloying elements Mg, Ca and Sr*, Mater. Des. vol.83, pp. 95–102, 2015, doi: [10.1016/j.matdes.2015.05.089](https://doi.org/10.1016/j.matdes.2015.05.089)
- [14] V. O. Oanca, *Techniques for optimizing the resistance to cavitation erosion of some CuAlNiFeMn alloys intended for the execution of naval propellers*, PhD thesis, Timisoara, Romania, 2014
- [15] ASTM G 32-016, *Standard Test Method for Cavitation Erosion Using Vibratory Apparatus*, ASTM International West Conshohocken, PA, USA, 2016
- [16] I. Mitelea, I. Bordeasu, E. Riemschneider, I. D. Utu, C. M. Craciunescu, *Cavitation erosion improvement following TIG surface-remelting of gray cast iron*, Wear 2022, art. number 204282, pp.496–497, 2022, doi: [10.1016/j.wear.2022.204282](https://doi.org/10.1016/j.wear.2022.204282)
- [17] I. Istrate, B. G.Sarcea, A. M. Demian, A. D. Buzatu, L. Salcianu, I. Bordeasu, L.M. Micu, C. Ghera, B. Florea, B. Ghiban, *Correlation between Mechanical Properties - Structural Characteristics and Cavitation Resistance of Cast Aluminum Alloy type 5083*, Crystals, vol. 12, no.11, 2022, doi: [10.3390/cryst12111538](https://doi.org/10.3390/cryst12111538)
- [18] I. Mitelea, I. Bordeasu, D. Cosma, I. D. Utu, C. M. Craciunescu, *Microstructure and Cavitation Damage Characteristics of GX40CrNiSi25-20 Cast Stainless Steel by TIG Surface Remelting*, Materials, vol. 16, no.4, art.number 1423, 2023, doi: [doi.org/10.3390/ma16041423](https://doi.org/10.3390/ma16041423)
- [19] I. Bordeasu, C. Patrascioiu, R. Badarau, L. Sucitu, M. Popoviciu, V. Balasoiu, *New contributions in cavitation erosion curves modeling*, FME Transactions Faculty of Mechanical Engineering, New Series, vol. 34, Nr.1/2006, YU ISSN 1451-2092, University of Belgrade, pp. 39-44, 2006



- [20] L. M. Micu, I. Bordeasu, M.O. Popoviciu, *A New Model for the Equation Describing the Cavitation Mean Depth Erosion Rate Curve*, Revista de Chimie, vol.68, no.4, pp 894-898, 2017, doi: [10.37358/RC.17.4.5573](https://doi.org/10.37358/RC.17.4.5573)
- [21] A.D. Jurchela, *Cercetări asupra eroziunii produse prin cavitație vibratorie la oțelurile inoxidabile cu conținut constant în crom și variabil de nichel*, PhD thesis, Timisoara, Romania, 2012
- [22] I. Bordeasu, *Eroziunea cavitationala a materialelor*, Editura Politehnica Timisoara, 2006

Article in Press